# Self-consistent and exact studies of pairing correlations and crossover in the one-dimensional attractive Hubbard model

A. N. Kocharian
*Department of Physics and Astronomy, California State University, Northridge, California 91330*

C. Yang
*Department of Physics, Tamkang University, Tamsui, Taiwan 251, Republic of China*

Y. L. Chiang
*Department of Physics, Chinese Culture University, Taipei, Taiwan 111, Republic of China*
*and Department of Physics, Tamkang University, Tamsui, Taiwan 251, Republic of China*
(Received 13 July 1998)

Ground-state properties of the attractive Hubbard model in one dimension are studied by means of both the exact Bethe-ansatz formalism and the self-consistent field (SCF) approach with renormalized chemical potential for general band fillings $n$ and a wide range of coupling strength $U/t$. The energy, the concentration of double occupied sites, the kinetic energy and the chemical potential of the ground state are in a good numerical agreement with the exact results over a wide range of parameters $U/t$ and $n$. The concentration of local pairs or double occupied sites in the Bethe-ansatz solution serves as a suitable parameter measuring the electron pairing correlations. The SCF theory provides a simple analytical relationship between the concentration of double occupied sites, the band filling and the BCS order parameter, valid for arbitrary $U/t$ and $n$. The calculated energy gap, the BCS order parameter, the phase diagram and the compressibility are also discussed. The SCF theory in one dimension distinguishes the order parameter from the excitation gap and suggests a smooth crossover away from half-filling (at $n \neq 1$) from the BCS pairing to the Bose condensation regime under the variation of $U/t$ and $n$. [S0163-1829(99)04911-5]

## I. INTRODUCTION

The attractive Hubbard model (see, e.g., Ref. 1) exhibits the simplest Hamiltonian that incorporates the basic ingredients of electron pairing correlations in lattices, and because of its controllable coupling strength $U/t$, is frequently applied in a weak-coupling (BCS theory[2,3]) and a strong-coupling (model of local pairs[4–6]) regimes to explain the appearance of the superconductivity and the charge-density waves in conventional and new high-temperature superconductors.[7,8] The exact solution of this model in one dimension[9–12] provides reliable information on the general features of electron pairing and can serve as a benchmark for approximate theories for the intermediate region of $U/t$. It is interesting to compare the predictions of the self-consistent field (SCF) approach (or modified BCS approach where the variation of particles is included and the weak coupling regime is not assumed) with the exact Bethe-ansatz results in a wide range of the coupling strength and for all band fillings.[13,14]

The gas of electrons in continuum model interacting via attractive potential displays a crossover from the strong-coupling extreme of tightly bound weakly interacting local Bose pairs (composite bosons) to the weak-coupling limit of relatively large overlapping Cooper pairs.[15,16] The crossover between the BCS pairing and the Bose condensation regimes has been a subject of many recent works.[17–19] In Ref. 15, this intriguing question for the continuum model of a Fermi gas with a fictitious separable attractive potential has been analyzed. As far as we know, the existence of the crossover from the BCS superconductivity to superfluidity of local pairs in a lattice driven by band filling and interaction strength is an open question. It is interesting to study the crossover in a discrete model under the variation of the number of electrons (or chemical potential) and to understand the peculiarity of one-dimensional system exactly at half-filling.

The purpose of this paper is to investigate the effect of the variation of band filling $n$ and coupling strength $-U/t$ on the ground-state properties in an attractive Hubbard model. The final goal is to develop a reliable self-consistent field theory over a wide range of $-U/t$. The lack of the exact results for many physical quantities even in one dimension leads to difficulties for systematic studies of approximate theories. In this paper we derive the exact integral Bethe-ansatz equations for the concentration of double occupied sites, the kinetic energy, the chemical potential, and the compressibility (the inverse of the charge susceptibility[20]), extending in this way previous exact results.[9,10,12,21,22] We test the SCF theory by numerically calculating the ground-state characteristics as functions of $-U/t$ or $n$ and comparing with our exact results.

Our investigations show that in two extremes (weak and strong coupling) the exact and self-consistent results are identical and they are also moderately close one to another at the intermediate coupling strength. We found that the SCF theory with renormalized chemical potential provides a simple and reasonable interpolation scheme between the weak and strong interaction limit for all band fillings. Even in one-dimensional case the SCF approach displays the crossover and the main ground-state features of very general

 

relevance. We expect that this theory will be even more accurate in higher dimensions, where the quantum fluctuations become significantly suppressed.

Although the attractive Hubbard model is similar to the one-dimensional electron gas with pairwise attractive $\delta$-function interaction in the continuum model,[13,23] there are some specific features related with a lattice model exactly at half-filled band. The crossover from a weak- to a strong-coupling superconductivity for different concentrations of electrons within the SCF theory is studied by comparison with the exact results. There is extensive evidence, direct[24] and indirect,[25] for the local quasi-one-dimensional character of electronic structure in high temperature superconductors. Unlike the conventional superconductors in which the phase coherence and pairing occur at once and at same temperature, in the underdoped cuprates there exists a separation between the pair binding and superconductivity as doping is decreased below the optimal value.[26] It is also well established that the pseudogap in a normal state has essentially the same magnitude and momentum dependence as in the superconducting state.[27] The evolution of the energy gap (Fermi surface in the momentum space) with the band filling and the coupling strength in the SCF approach are also examined. The interplay between the Bose condensation and localization of electrons with purely attractive interaction are discussed in the context of the existence of a pseudogap in the insulating state of underdoped cuprates at vanishing carriers concentration.[28] In general separation between the binding and phase coherence can be accomplished either by increasing the coupling strength or by decreasing the density of electrons. We study the pair formation associated with the distinct change in the band structure driven by both $U/t$ and $n$. Our simplified model with local attraction which does not have all the features of real superconductors, nevertheless provides a reasonable testing ground for approximate approaches intended for the full problem.

The paper is organized as following: After an introduction (Sec. I) we review the model and the basic formalism for the SCF approach (Sec. II) and the solution of the Bethe-ansatz equations (Sec. III). Section IV presents the numerical calculations of the ground-state properties and a comparison between the exact and the SCF results, using both the Bethe-ansatz and the SCF approach. Section V constitutes a summary. The Appendixes deal with the exact calculation schemes (integration equations) for the concentration of local pairs, the kinetic energy, the chemical potential, the energy gap, the compressibility, and the SCF calculation scheme (self-consistent equations) for the compressibility.

## II. ATTRACTIVE ELECTRONS IN LATTICE AND THE SCF APPROACH

The model under consideration is the Hubbard model defined by the Hamiltonian

$$H=-t\sum_{\langle i,j\rangle,\sigma} c_{i\sigma}^{+}c_{j\sigma}+U\sum_{i} c_{i\uparrow}^{+}c_{i\downarrow}^{+}c_{i\downarrow}c_{i\uparrow}, \tag{1}$$

where $t>0$ corresponds to the kinetic energy of electron hopping between two nearest neighbors $i$ and $j$, $\sigma=\pm 1$ ($\uparrow$ or $\downarrow$) is the spin index, $U$ is the coupling strength ($U<0$), and $c_{i\sigma}^{+}$ ($c_{i\sigma}$) is the Fermi creation (destruction) operator of an electron at site $i$ with spin $\sigma$.

After Fourier transformation the Hamiltonian takes the form

$$H=\sum_{\mathbf{k},\sigma} \varepsilon_{\mathbf{k}}c_{\mathbf{k}\sigma}^{+}c_{\mathbf{k}\sigma}+\frac{U}{N_{\mathrm{latt}}}\sum_{\mathbf{k},\mathbf{k}',\mathbf{Q}} c_{\mathbf{k}+\mathbf{Q}\uparrow}^{+}c_{\mathbf{k}'-\mathbf{Q}\downarrow}^{+}c_{\mathbf{k}\downarrow}c_{\mathbf{k}'\uparrow}, \tag{2}$$

where $N_{\mathrm{latt}}$ is the total number of lattice sites,

$$\varepsilon_{\mathbf{k}}=-t\sum_{\mathbf{R}} \exp(i\mathbf{k}\cdot\mathbf{R}), \tag{3}$$

$\mathbf{R}\equiv\mathbf{r}_i-\mathbf{r}_j$ is the nearest-neighbor vector. In one dimension ($R=1$) $\varepsilon_{\mathbf{k}}=-2t\cos k$.

The average number of electrons (or band filling) $n$, the average spin $s$, and the BCS order parameter $\Delta$ are defined as

$$n=\frac{1}{N_{\mathrm{latt}}}\sum_{\mathbf{k},\sigma}\langle c_{\mathbf{k}\sigma}^{+}c_{\mathbf{k}\sigma}\rangle, \quad \sigma=\pm 1(\uparrow \text{ or } \downarrow), \tag{4}$$

$$s=\frac{1}{2N_{\mathrm{latt}}}\sum_{\mathbf{k},\sigma}\sigma\langle c_{\mathbf{k}\sigma}^{+}c_{\mathbf{k}\sigma}\rangle, \tag{5}$$

$$\Delta=\frac{2U}{N_{\mathrm{latt}}}\sum_{\mathbf{k}}\langle c_{\mathbf{k}\uparrow}c_{-\mathbf{k}\downarrow}\rangle. \tag{6}$$

In the SCF approach we introduce the consistent chemical potential $\mu$, which must be adjusted to fix the band filling $n$, and use the canonical transformation method (see, e.g., Refs. 29 and 30) to diagonalize the Hamiltonian by means of the new operators

$$b_{\mathbf{k}\uparrow}=u_{\mathbf{k}}c_{\mathbf{k}\uparrow}-v_{\mathbf{k}}c_{-\mathbf{k}\downarrow}^{+},$$

$$b_{-\mathbf{k}\downarrow}=u_{\mathbf{k}}c_{-\mathbf{k}\downarrow}+v_{\mathbf{k}}c_{\mathbf{k}\uparrow}^{+}, \tag{7}$$

where $u_{\mathbf{k}}$ and $v_{\mathbf{k}}$ are real coefficients that satisfy the normalization condition

$$u_{\mathbf{k}}^{2}+v_{\mathbf{k}}^{2}=1. \tag{8}$$

Minimization of the total energy with respect to $u_{\mathbf{k}}$ and $v_{\mathbf{k}}$ gives the following results (see, e.g., Refs. 29 and 30):

$$u_{\mathbf{k}}^{2}=\frac{1}{2}\left(1+\frac{\varepsilon_{\mathbf{k}}-\overline{\mu}}{E_{\mathbf{k}}}\right), \tag{9}$$

$$v_{\mathbf{k}}^{2}=\frac{1}{2}\left(1-\frac{\varepsilon_{\mathbf{k}}-\overline{\mu}}{E_{\mathbf{k}}}\right), \tag{10}$$

$$E_{\mathbf{k}}=\sqrt{(\varepsilon_{\mathbf{k}}-\overline{\mu})^{2}+\frac{\Delta^{2}}{4}}, \tag{11}$$

we have the SCF Hamiltonian for quasiparticles

$$H_{\mathrm{SCF}}=\sum_{\mathbf{k},\sigma} E_{\mathbf{k}}b_{\mathbf{k}\sigma}^{+}b_{\mathbf{k}\sigma}+N_{\mathrm{latt}}(E_{\mathrm{GS}}-\mu n), \tag{12}$$

where

$$E_{\mathrm{GS}}-\mu n=\frac{2}{N_{\mathrm{latt}}}\sum_{\mathbf{k}}(\varepsilon_{\mathbf{k}}-\bar{\mu})v_{\mathbf{k}}^2 - \frac{\Delta}{N_{\mathrm{latt}}}\sum_{\mathbf{k}}u_{\mathbf{k}}v_{\mathbf{k}}-\frac{\Delta^2}{4U}-\frac{n^2}{4}U \tag{13}$$

is the ground-state average value $\langle H_{\mathrm{SCF}}\rangle$ per one lattice site, and

$$\bar{\mu}\equiv\mu-\frac{nU}{2} \tag{14}$$

is the renormalized chemical potential in the SCF approach.

In the SCF approach the number of electrons $n$ and the BCS order parameter $\Delta$ are included on an equal footing, and by minimization of $E_{\mathrm{GS}}-\mu n$ over these parameters, one can obtain a set of self-consistent equations[14] determining $n$ and $\Delta$ at a given $\mu$ (or $\mu$ and $\Delta$ at a given $n$):[16]

$$\frac{1}{N_{\mathrm{latt}}}\sum_{\mathbf{k}}\frac{\varepsilon_{\mathbf{k}}-\bar{\mu}}{E_{\mathbf{k}}}=1-n, \tag{15}$$

$$\frac{U}{N_{\mathrm{latt}}}\sum_{\mathbf{k}}\frac{1}{2E_{\mathbf{k}}}=-1. \tag{16}$$

Note that at half-filling ($n=1$) $\bar{\mu}=0$, and we restore the usual BCS result for $\Delta$. After simple algebraic transformations, the ground-state energy in Eq. (13) can be written in a more convenient form

$$E_{\mathrm{GS}}=-\frac{1}{N_{\mathrm{latt}}}\sum_{k}E_{\mathbf{k}}+\frac{n^2U}{4}-\frac{\Delta^2}{4U}-\bar{\mu}(1-n). \tag{17}$$

In the thermodynamic limit $N_{\mathrm{latt}}\gg 1$, the sum over $\mathbf{k}$ can be replaced by an integral over the first Brillouin zone.

## III. LIEB-WU EQUATIONS

The Bethe-ansatz technique[9,12,14] gives an exact solution of the Hubbard model (1) in one dimension. In the limit $N_{\mathrm{latt}}\gg 1$, the energy of the system per one lattice site is

$$E=U\left(\frac{n}{2}-s\right)-2t\int_{-Q}^{Q}dk\rho(k)\cos k, \tag{18}$$

where $0\leqslant n\leqslant 1$, $0\leqslant s\leqslant n/2$ and $\rho(k)$ is determined from the Fredholm integral equations

$$\rho(k)=\frac{1}{2\pi}-\frac{U\cos k}{4t\pi}\int_{-B}^{B}d\lambda\,\sigma(\lambda)f_1(k,\lambda), \tag{19}$$

$$\sigma(\lambda)=-\frac{U}{4t\pi}\int_{-Q}^{Q}dk\rho(k)f_1(k,\lambda) + \frac{U}{2t\pi}\int_{-B}^{B}d\lambda'\sigma(\lambda')f_2(\lambda,\lambda'), \tag{20}$$

$$f_1(k,\lambda)\equiv\frac{1}{(U/4t)^2+(\lambda-\sin k)^2}, \tag{21}$$

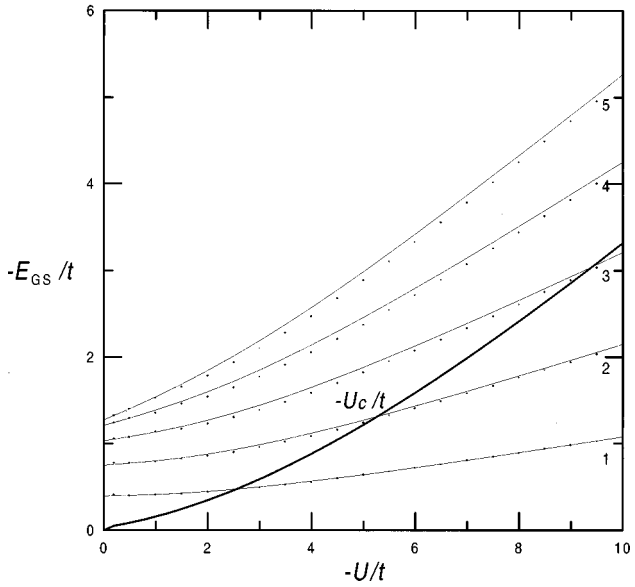


FIG. 1. The ground-state energy $E_{\mathrm{GS}}$ as a function of coupling strength $-U/t$ in the exact theory (solid curves) and the SCF approach (dots). Curve indexes 1–5 correspond to the values $n=0.2,0.4,0.6,0.8,1$. The bold curve indicates the smooth crossover from the BCS regime into the local pair behavior (see Sec. IV E).

$$f_2(\lambda,\lambda')\equiv\frac{1}{(U/2t)^2+(\lambda-\lambda')^2}, \tag{22}$$

with normalization conditions determining $Q$ and $B$,

$$\int_{-Q}^{Q}\rho(k)dk=1-2s, \tag{23}$$

$$\int_{-B}^{B}\sigma(\lambda)d\lambda=\frac{n}{2}-s. \tag{24}$$

The parameters $Q$ and $B$ generally depend on $n$, $s$, $U$, and $t$. The solution of Eqs. (18)–(24) at $s=0$ determines the exact ground-state energy

$$E_{\mathrm{GS}}=E|_{s=0}. \tag{25}$$

In this case $Q=\pi$ for all values of $U$, $t$, and $n$.

## IV. COMPARISON OF SCF AND EXACT GROUND-STATE RESULTS

### A. Energy

First we calculated the ground-state energy $E_{\mathrm{GS}}$ for the one-dimensional case in the SCF approach and in the exact theory according to the formulas (17) and (25), correspondingly. For this purpose we solved numerically the self-consistent equations (15) and (16) for given values of coupling strength $-U/t$ and band filling $n$ using an iteration algorithm. We also solved the integral equations (19) and (20) with the conditions (23) and (24) for the same values of $-U/t$ and $n$ using the subroutine *fred2* (see Ref. 31, §18.1). In Fig. 1, both results are shown as functions of $-U/t$ for different $n$. Similar results for the ground-state energy at $-U/t\leqslant 10$ have been reported previously in Ref. 14. In both

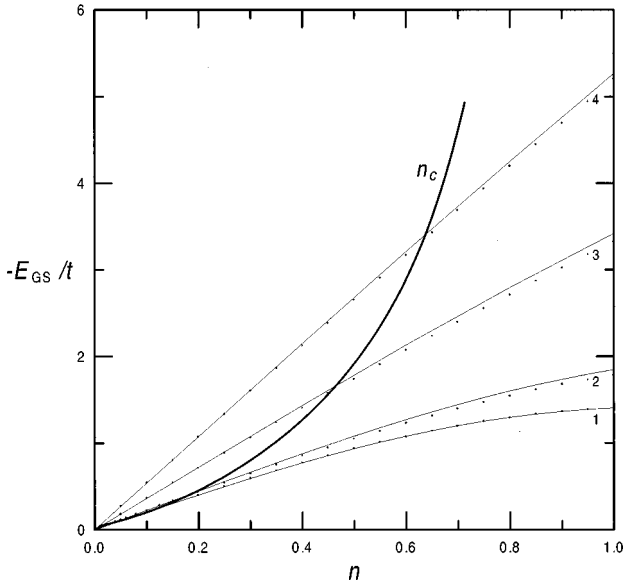


FIG. 2. The ground-state energy $E_{\mathrm{GS}}$ as a function of band filling $n$ in the exact theory (solid curves) and the SCF approach (dots). Curve indexes 1–4 correspond to the values $-U/t=0.5,2.0,6.0,10.0$. The bold curve indicates the crossover, as in Fig. 1.

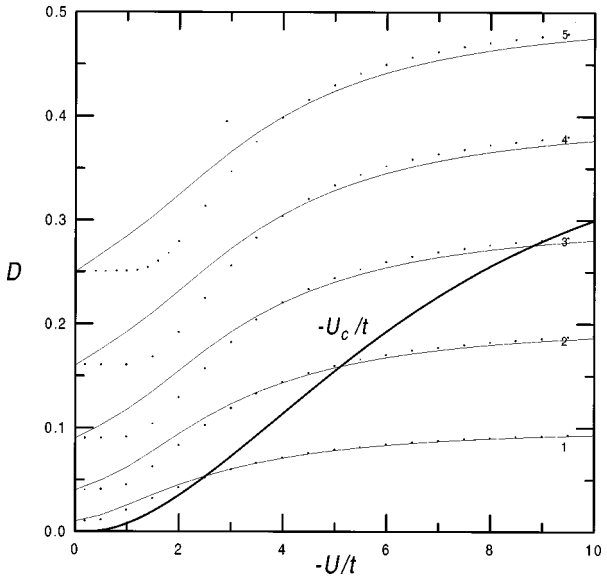


FIG. 3. The ground-state concentration of double occupied sites $D$ as a function of $-U/t$ in the exact theory (solid curves) and the SCF approach (dots). The indexes 1–5 and the bold curve mean the same as in Fig. 1.

extreme cases of strong and weak interaction the agreement between the exact and the SCF results is excellent, and a small deviation from the exact result occurs only near half-filled band ($n=1$) for intermediate values of $-U/t$. Note that the SCF approach gives a good numerical agreement with the exact result for various $n$. This conclusion is justified in Fig. 2, where the ground-state energy is shown as a function of $n$ for various values of $-U/t$. One can see from Fig. 2 that the ground-state energy in the SCF and the exact results both depend on $n$ linearly. Analytical calculations performed at a small concentration of electrons $n\rightarrow 0$ show that the SCF result coincides with the exact ground-state energy

$$E_{\mathrm{GS}}=-n\sqrt{\frac{U^2}{4}+4t^2} \tag{26}$$

for all values of $U/t$. This result in SCF approach is consistent with predictions of crossover and Bose condensation in the dilute regime (see Secs. IV E and IV G). The bold curves in Figs. 1 and 2 show the crossover from the BCS-like behavior into the Bose-Einstein condensation of local pairs (for an explanation see Sec. IV G). Note that in Fig. 2 the bold curve at small $n$ shows the crossover from linear dependency to a quadratic behavior. The system is in the BCS regime above and below the bold curve on Figs. 1 and 3, respectively. The bold curve in Fig. 1 does not intersect the curve for $n=1$, showing the stability of the half-filling case against the crossover into the Bose condensation regime.

### B. Concentration of double occupied sites

The concentration of the local pairs (or the double occupied sites) $D$ is a much more sensitive measure of pairing correlations than the ground-state energy. We define the concentration of the double occupied sites $D$ as

$$D\equiv\frac{1}{N_{\mathrm{latt}}}\sum_i\langle c_{i\uparrow}^{+}c_{i\uparrow}c_{i\downarrow}^{+}c_{i\downarrow}\rangle. \tag{27}$$

Obviously [see Eq. (1)], this quantity measures the derivative of energy with respect to $U$,

$$D=\frac{\partial\langle H\rangle}{N_{\mathrm{latt}}\partial U}=\frac{\partial E}{\partial U}, \tag{28}$$

where $E\equiv\langle H\rangle/N_{\mathrm{latt}}$.

In the exact theory we can calculate $D$ from Eq. (18) (see Appendix A). For the SCF approach, the parameter $D$ can be derived from Eq. (17). It is not difficult to find out that at $U=0$ we have

$$D=D_0\equiv\frac{n^2}{4}. \tag{29}$$

From Eqs. (28), (17), and (15) we find that the SCF approach gives the common relationship between the concentration of double occupied sites $D$, the BCS order parameter $\Delta$, and the filling factor $n$,

$$D=D_0+\frac{\Delta^2}{4U^2}, \tag{30}$$

valid for arbitrary $U<0$ and all $n$ values. The order parameter $\Delta$ in Eq. (30) is found self-consistently from the Eqs. (15) and (16) depending on $n$ and $-U/t$. The coupling strength and the band filling favors the formation of local pairs and double occupancy of sites. For general band filling $0\leqslant n\leqslant 2$ the parameter $D$ is changed in the range $0\leqslant D\leqslant 1$. The term $\Delta^2/4U^2$ in Eq. (30) shows the probability for a pair of electrons to be found in a local bound state and the average quantity (27) has a meaning of total probability for electrons to be in a form of local pairs (both bound and unbound).

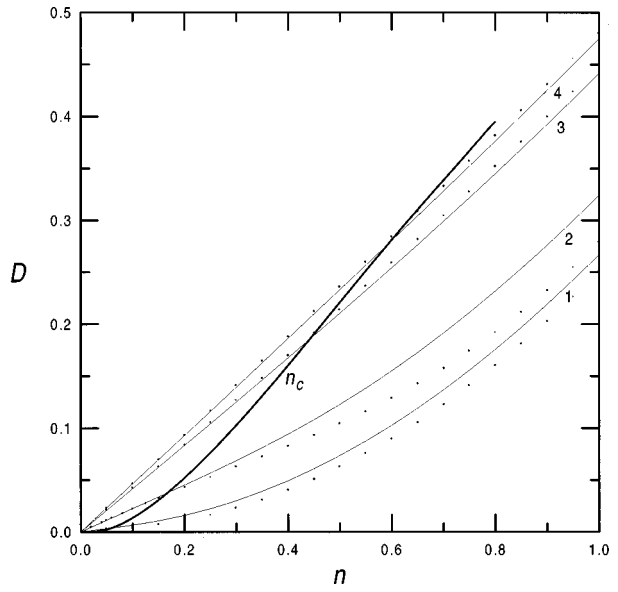


FIG. 4. The ground-state concentration of double occupied sites $D$ as a function of $n$ in the exact theory (solid curves) and the SCF approach (dots). The indexes 1–4 and the bold curve mean the same as in Fig. 2.

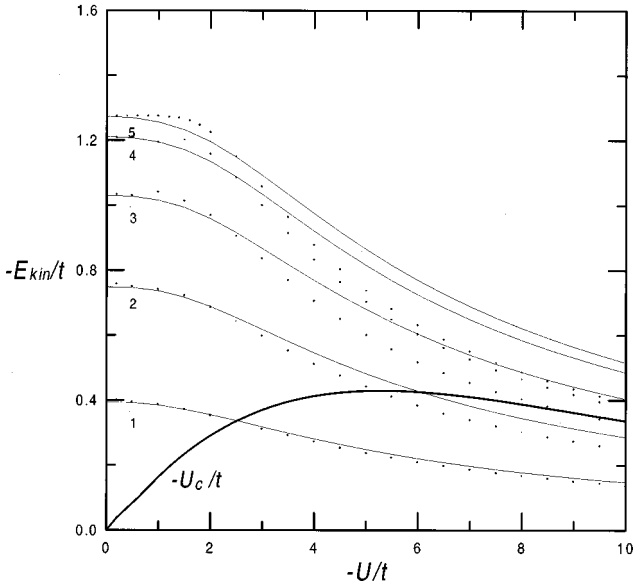


FIG. 5. The ground-state kinetic energy $E_{\rm kin}$ as a function of $-U/t$ in the exact theory (solid curves) and the SCF approach (dots). The indexes 1–5 and the bold curve mean the same as in Fig. 1.

In Fig. 3 we compare the exact Bethe ansatz and the SCF results for $D$ values in the ground state as functions of $-U/t$ for different $n$. One can see that the SCF data follow the exact result much more closely at large values of $-U/t$, while the maximum deviation occurs at small values of $-U/t$ near the half-filled band. The SCF result for $D$ barely changes at weak coupling $-U/t \ll 1$, while the exact result gives a linear dependence. We see from Fig. 3 that the SCF results for $D$ underestimate the local pairing correlations at small $-U/t$. Hence the derivative of $D$ with respect to $-U$ (positive slope) measures the degree to which pairing correlations are included in the SCF approach at the weak-coupling limit. Thus, the correlation effect in the SCF approach becomes ineffective for relatively small values $U/4t \ll 1$. In contrast, at large $-U/t$ values the SCF approach suppresses the fluctuations and therefore slightly overestimates the exact $D$ values.

For comparison in Fig. 4 we show the concentration of double occupied sites as a function of $n$ for various values of $-U/t$. Again we see the parameter $D$ increases monotonically with $-U/t$ increasing at a given $n$ and with $n$ increasing at a given $-U/t$. In the SCF approach $\Delta$ is exponentially small at weak coupling and $D \approx D_0$. At strong coupling, $\Delta = |U|\sqrt{n(2-n)}$ (Ref. 32) and the concentration of double occupied sites becomes equal to the number of local pairs $D \approx n/2$. Thus the SCF result for the parameter $D$ interpolates between the number of itinerant ($n^2/4$) and local pairs ($n/2$) by increasing the coupling strength $-U/t$. In Figs. 3 and 4 the bold curves show the smooth crossover from BCS-like superconductivity to a strong-coupling Bose condensation by increasing $|U|/t \geqslant |U|_c/t$ and decreasing $n \leqslant n_c$, respectively. The exact results for $D$ are remarkably well reproduced within the SCF approach with renormalized chemical potential, especially at large and small $-U/t$. Based on the common SCF relationship (30) and a reasonable agreement with the exact results we conclude that the parameter $D$ may serve as a reliable measure of pairing correlations for general band filling and over wide range of $-U/t$.

### C. Kinetic energy

The kinetic energy,

$$E_{\rm kin} \equiv -\frac{t}{N_{\rm latt}} \sum_{\langle i,j\rangle,\sigma} \langle c^+_{i\sigma} c_{j\sigma} \rangle, \tag{31}$$

also serves as a measure for estimation of electron pairing correlations. From Eqs. (1) and (27) we have an exact relation between $E_{\rm kin}$ and $D$,

$$E_{\rm kin} = E - UD. \tag{32}$$

Otherwise, we may calculate the kinetic energy by differentiating the total energy with respect to $t$,

$$E_{\rm kin} = t\frac{\partial E}{\partial t}. \tag{33}$$

We can calculate $E_{\rm kin}$ in the exact theory resolving corresponding integral equations (Appendix B). For the SCF approach, using Eq. (17), we have in the ground state

$$E_{\rm kin} = \frac{1}{N_{\rm latt}} \sum_k \frac{(\varepsilon_{\mathbf{k}} - \overline{\mu})\varepsilon_{\mathbf{k}}}{\sqrt{(\varepsilon_{\mathbf{k}} - \overline{\mu})^2 + \Delta^2/4}}. \tag{34}$$

Figure 5 presents ground state $E_{\rm kin}/t$ as a function of the coupling strength $-U/t$ for various $n$. The SCF result for $E_{\rm kin}$ is more accurate at weak coupling comparing with the corresponding result for parameter $D$ shown in Fig. 3. The exact and the SCF results show significant narrowing of the effective bandwidth by increasing $U/t$. The SCF approach overestimates the effect of pairing correlation in the kinetic energy at weak coupling and underestimates it at strong cou-

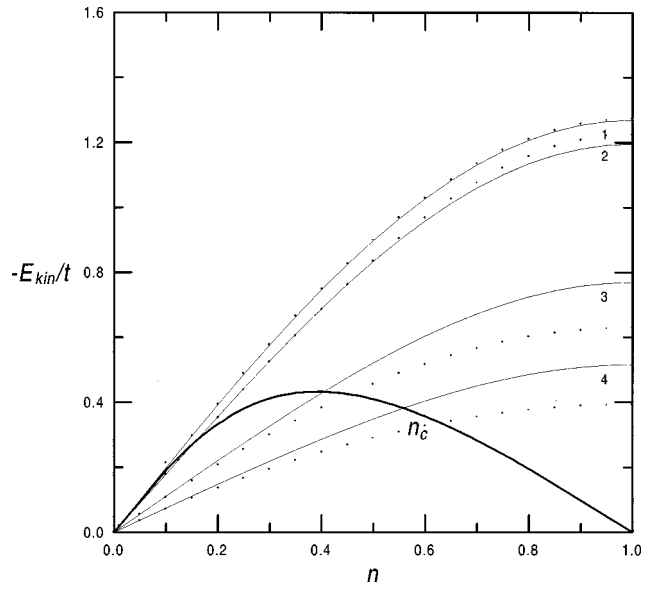


FIG. 6. The ground-state kinetic energy $E_{\rm kin}$ as a function of $n$ in the exact theory (solid curves) and the SCF approach (dots). The indexes 1–4 and the bold curve mean the same as in Fig. 2.

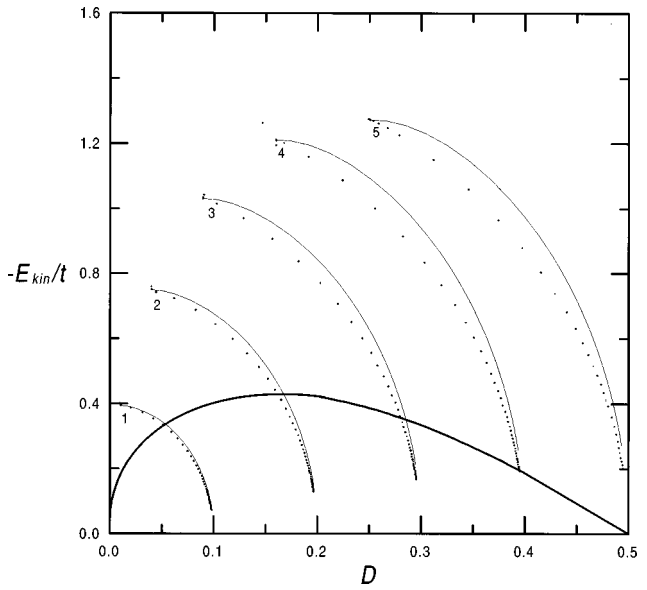


FIG. 7. The ground-state kinetic energy $E_{\rm kin}$ as a function of $D$, when $-U/t$ is changed, in the exact theory (solid curves) and the SCF approach (dots). The indexes 1–5 and the bold curve mean the same as in Fig. 1.

pling. The SCF approach becomes ineffective at small $U/t$ values and the maximum deviation from the exact results occurs at the half-filling case for intermediate coupling strength. In Fig. 6 we plot $E_{\rm kin}/t$ as a function of the band filling $n$ for various $-U/t$ values. We notice that the effective bandwidth gradually diminishes with decreasing band filling $n$ and it is significantly suppressed (narrowed) at strong-coupling limit near zero filling $(n\rightarrow 0)$. The suppression of the bandwidth at vanishing carrier concentration reminds the trivial metal-insulator transition. A good agreement with the exact results is obtained at small $n$ and large $-U/t$. The bold curve in Figs. 5 and 6 indicates the pair formation vs condensation in kinetic energy. The smooth crossover from the BCS into the Bose condensation regime occurs below the bold curve in Fig. 5 and above it in Fig. 6 at the cross points with corresponding curves.

To better illustrate the correlations in behavior between the concentration of double occupied sites $D$ and the kinetic energy $E_{\rm kin}$, we present the dependence of $E_{\rm kin}/t$ versus $D$ for the exact and the SCF results when the coupling strength changes at different given values of $-U/t$ (Fig. 7) and when the band filling changes at different given values of $n$ (Fig. 8). In Figs. 7 and 8 the intersections of the SCF results with the bold curve show the crossover from the BCS regime (above the curve) into the Bose condensation phase (below the curve). The agreement between the results is quite well at weak and strong couplings. Note that the agreement is good at $n\leqslant 0.2$ also for intermediate coupling (Fig. 7) and at $-U/t\leqslant 0.5$ for all values of $n$ (Fig. 8). The area below the bold curve presents the BCS-like behavior in Fig. 7 and the Bose condensation regime in Fig. 8.

### D. Chemical potential

The chemical potential is also an important characteristic for the evaluation of the SCF theory. From Bethe-ansatz equations one can calculate the exact chemical potential

$$\mu=\frac{\partial E}{\partial n} \tag{35}$$

(see Appendix C). From SCF Eqs. (15) and (16) one can numerically determine the SCF chemical potential. In Fig. 9 the ground-state chemical potential values are plotted for all values of $-U/t$ and different band fillings $n$. At half-filling $(n=1)$ $\mu=-|U|/2$ for all values of $U$. In an empty band (at zero filling, $n=0$)

$$\mu=\mu_{\rm zero}\equiv-\sqrt{\frac{U^2}{4}+4t^2} \tag{36}$$

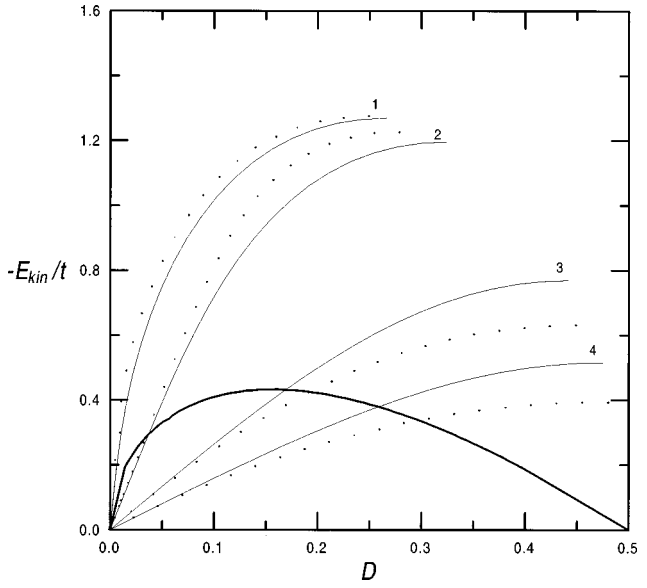


FIG. 8. The ground-state kinetic energy $E_{\rm kin}$ as a function of $D$, when $n$ is changed, in the exact theory (solid curves) and the SCF approach (dots). The indexes 1–4 and the bold curve mean the same as in Fig. 2.

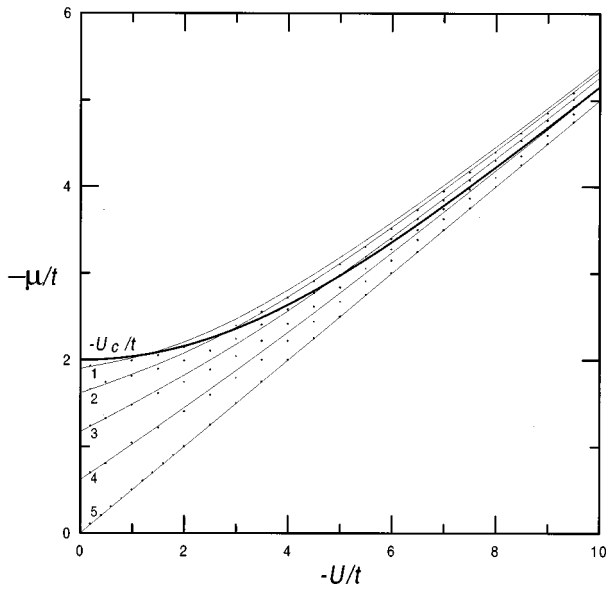


FIG. 9. The ground-state chemical potential $\mu$ as a function of $-U/t$ for various $n$ in the exact theory (solid curves) and the SCF approach (dots). The indexes 1–5 and the bold curve mean the same as in Fig. 1.

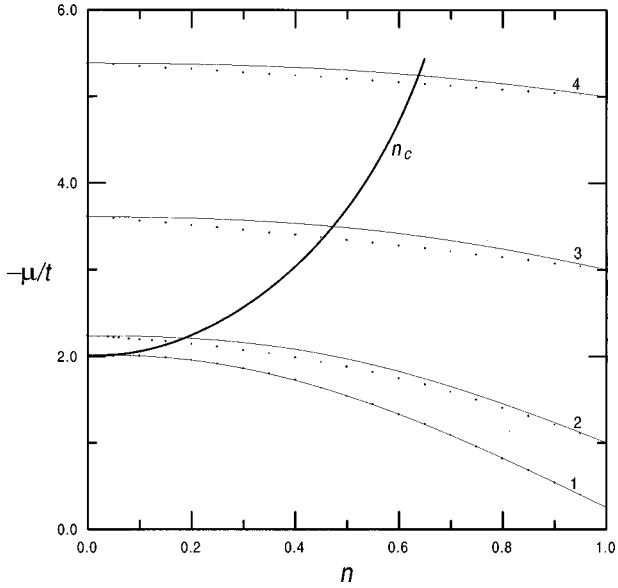


FIG. 10. The ground-state chemical potential $\mu$ as a function of $n$ for various $-U/t$ in the exact theory (solid curves) and the SCF approach (dots). The indexes 1–4 and the bold curve mean the same as in Fig. 2.

(Ref. 33) and the SCF results for $\mu$ coincide with the exact ones. We have a good agreement also for intermediate values of $n$ and for various $-U/t$ values. For $n \ll 1$ and $|U|/t \ll 1$ the chemical potential $\mu$ decreases (algebraically) approximately as $-U^2$. This result is consistent with the corresponding exact result for continuum model of excitonic insulator.[34] In another limit ($n > n_c$ and $|U|/t \ll 1$) the dependence of $\mu$ on $U/t$ in the SCF approach is linear $\mu = (nU/2) - 2t\cos(n\pi/2)$. The bold curve in Fig. 9 indicates the transition from the BCS regime (below the curve) into the Bose condensation (above the curve) under variation of the parameter $-U/t$ (see Secs. IV E and IV G). Note that the SCF curve of $\mu$ for $n=1$ in Fig. 9 everywhere is below the bold curve, showing that the system at half-filling remains in the BCS regime even at large $-U/t$ values.

Figure 10 shows the variation of ground-state $\mu/t$ as a function of $n$ for various $-U/t$. Note that $\mu$ increases (algebraically) monotonically with the band filling ($d\mu/dn > 0$) providing the stability of the pairing phase[15] (the compressibility is positive). The SCF chemical potential coincides with the exact one in the two extreme cases of strong and weak coupling and is moderately close to the exact solution for intermediate values of $-U/t$. At $U=0$ we have a simple relationship between the chemical potential and band filling, $\mu = -2t\cos(n\pi/2)$ and a metal-insulator transition occurs when $\mu$ approaches the bottom of the band $\mu = -2t$. This gives the simple relation between $\mu$ and $n$ near the band edge $n = \pi^{-1}\sqrt{4+2\mu/t}$. The SCF result nicely follows the exact one for all $-U/t$ and we find a smooth transition from quadratic behavior $\mu \propto n^2$ at weak coupling to a linear dependence $\mu \propto n$ at the strong-coupling limit. At large $|U|/t$ it readily follows from Eqs. (15) and (16) that to the order of $t^2/|U|$ we have approximately a linear dependence,

$$\mu = \frac{U}{2} + \frac{4t^2(1-n)}{U}. \tag{37}$$

In Fig. 10 the bold curve displays the crossover under the variation of $n$ from the BCS-like (below the curve) into the Bose-Einstein behavior (above the curve). Finally we should stress that the numerical agreement between the exact and approximate results for $\mu$ in a discrete lattice is much more accurate than for the corresponding result for $\mu$ in a continuum model.[13]

### E. Energy gap

For further corroboration of the validity of the SCF approach we compare the results for the energy gap. In the SCF approach the order parameter $\Delta$ and the single-particle excitation energy gap $E_{\rm gap} \equiv 2\min E_k$ are determined by Eq. (11) and both vary with $n$. At half-filling ($n=1$) we find from Eqs. (15) and (16) that the minimum excitation gap, which occurs at $k = k_0 = \pi/2$, is equal to the order parameter $E_{\rm gap} = \Delta$. At $n<1$ the minimum excitation gap occurs at $k = k_0$ where

$$k_0 = \begin{cases} \arccos\left(-\dfrac{\overline{\mu}}{2t}\right), & \text{if } |\overline{\mu}| < 2t, \\ 0, & \text{if } |\overline{\mu}| \geq 2t. \end{cases} \tag{38}$$

In the first case $E_{\rm gap} = \Delta$. In the second case, possible only away from half-filling, the energy gap to break a pair is

$$E_{\rm gap} = \sqrt{4(\overline{\mu}+2t)^2 + \Delta^2} \tag{39}$$

and $E_{\rm gap}$ is generally greater than $\Delta$. Thus the equality

$$\overline{\mu} + 2t = 0 \tag{40}$$

determines the critical value $n_c$ of the band filling at a given $U/t$ (or the critical value $U_c/t$ of the coupling strength at a given $n$) showing that the energy gap and the SCF order parameter $\Delta$ are different whenever $n < n_c$ at fixed $-U/t$ (or whenever $|U|/t > |U_c|/t$ at given $n$). In spectrum near $\overline{\mu} =$

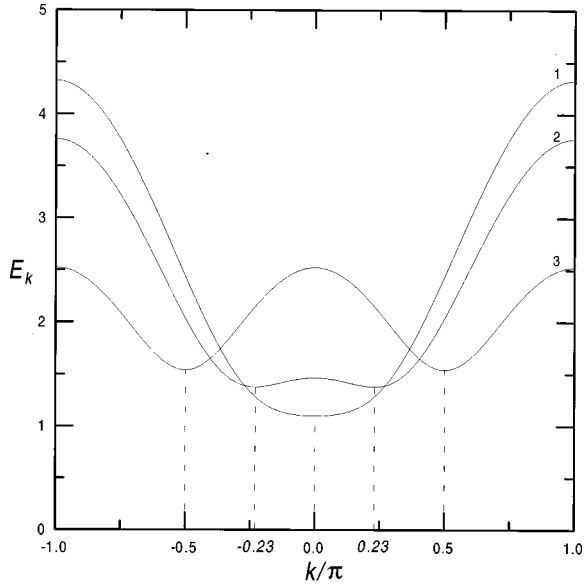


FIG. 11. The one-quasiparticle excitation energy spectrum in the SCF approach at $-U/t=4.0$. Curve indexes 1–3 correspond to $n=0.25,0.5,1.0$. The minimum excitation gap in momentum space with $k=0$ occurs at $n<n_c=0.32$ (see Fig. 16).

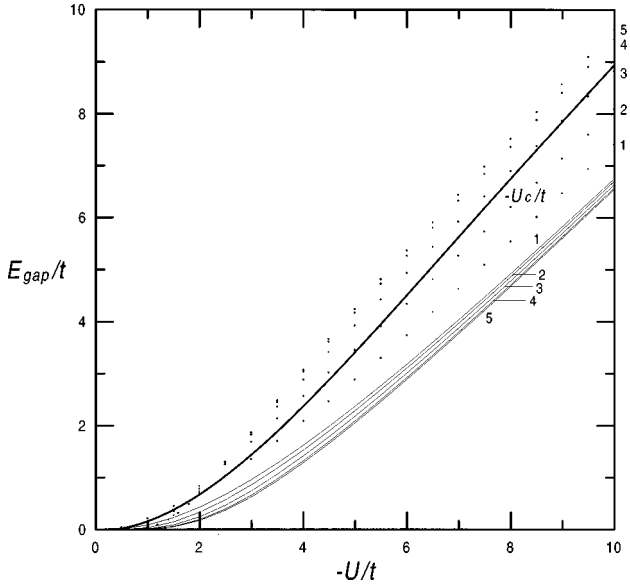


FIG. 12. The SCF energy gap $E_{\rm gap}$ as a function of $-U/t$ for various $n$. The indexes 1–5 and the bold curve mean the same as in Fig. 1.

$-2t$ there exists a weak singularity, which describes a smooth crossover by changing the parameters $U/t$ or $n$ from the BCS regime into a Bose condensate of structureless local bosonic pairs with total momentum $k=0$.[15] Note that at the crossover the renormalized chemical potential $\bar{\mu}$ driven by the couping strength or band filling approaches the bottom of the band $-2t$ and leads to the transition from the BCS-like into the Bose condensation behavior. This crossover closely resembles the onset of the localization of pairs at the insulator-metal transition in the case of vanishing carrier concentration $n\rightarrow 0$.

In Fig. 11 we show a quasiparticle energy spectrum at fixed $-U/t=4$ for three different values of $n$. The minimum excitation gap in the spectrum at $n=0.5$ occurs at the Fermi energy ($k_0=0.23\pi$). Below the critical value $n_c=0.32$, the minimum excitation gap occurs at $k_0=0$ and according to Eq. (39) the corresponding energy gap is greater than the order parameter $\Delta$.

Note that according to the generalized Luttinger theorem the position of singularity in the density-density correlation function is unrenormalized by the interaction strength and the corresponding parameter $k_F$ in a non-Fermi-liquid is the same as the Fermi momentum for $U=0$.[35,36] In contrast, the SCF result for the parameter $k_0$, which plays the similar role in single-particle spectrum for spin degrees of freedom, is renormalized by the interaction strength $-U/t$, only when $n\neq 1$.

In the exact solution the energy gap is determined as

$$E_{\rm gap}=\left.\frac{\partial E}{\partial(2s)}\right|_{s=+0}-\left.\frac{\partial E}{\partial(2s)}\right|_{s=-0} \tag{41}$$

and can be calculated from Eqs. (18)–(24) (see Appendix D).

The energy gap (or binding energy) in the exact and the SCF approaches has tendency to grow monotonously with increasing $-U/t$. In Fig. 12 we plot the dependence of $E_{\rm gap}/t$ versus $-U/t$ for different $n$. The variation of SCF gap $E_{\rm gap}/t$ with $n$ for various $U/t$ along with the exact result are given in Fig. 13. Near zero filling the exact gap increases slowly with the decreasing $n$, whereas the SCF gap slowly decreases with $n$. The bold curve in Figs. 12 and 13 indicates a smooth evolution of the SCF gap from the BCS regime into the Bose condensation regime by increasing of $U/t$ and $n$, respectively.

The exact and the SCF approaches at weak coupling both gives $E_{\rm gap}\propto t\exp(-2\pi t/|U|)$ at $n=1$, and $E_{\rm gap}\propto U^2/t$ at $n=0$. In a strong coupling within the SCF approach we have $E_{\rm gap}=|U|-4t^2/|U|$ at $n=1$ and $E_{\rm gap}=|U|-4t$ at $n=0$, while the exact solution gives $E_{\rm gap}=|U|-4t$ for all band fillings. The energy gap in weak coupling is reproduced

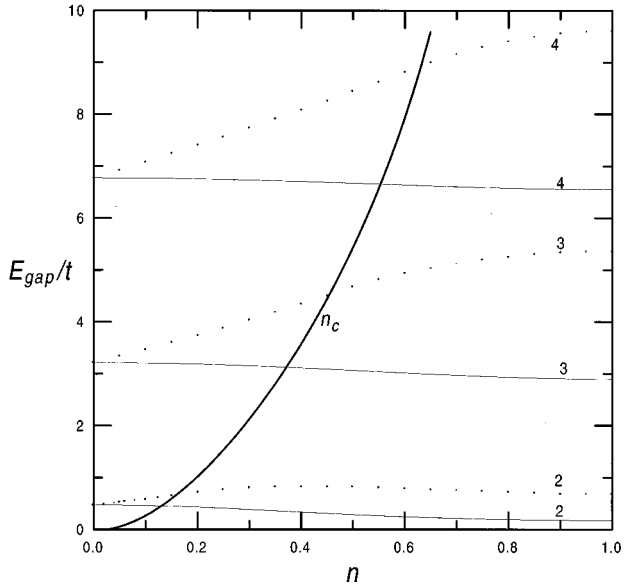


FIG. 13. The SCF energy gap as a function of $n$. The indexes 2–4 and the bold curve mean the same as in Fig. 2.

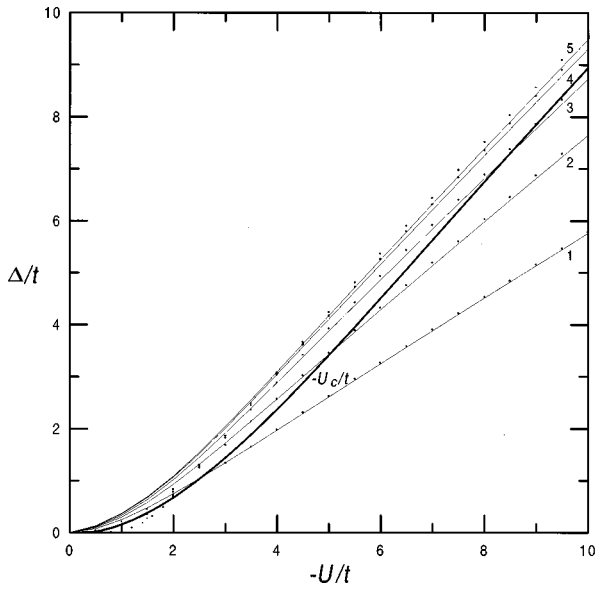


FIG. 14. The order parameter $\Delta$ as a function of $-U/t$ in the exact theory (solid curves) and the SCF approach (dots). The indexes 1–5 and the bold curve mean the same as in Fig. 1.

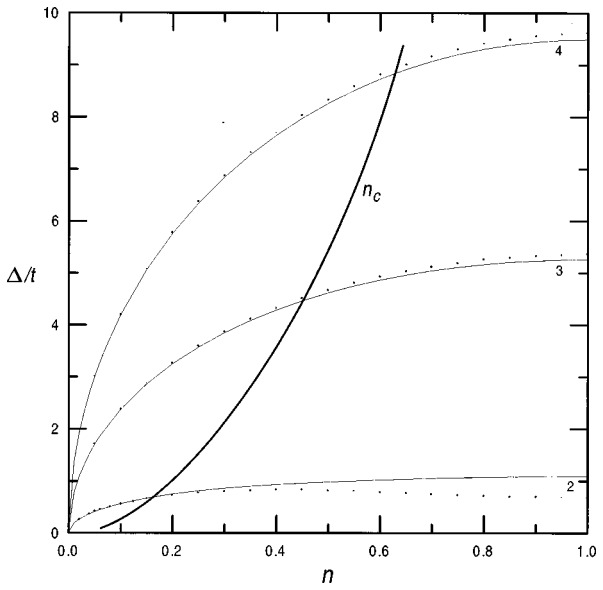


FIG. 15. The order parameter $\Delta$ as a function of $n$ in the exact theory (solid curves) and the SCF approach (dots). The indexes 2–4 and the bold curve mean the same as in Fig. 2.

rather well within the SCF approach and we expect to get even better agreement with the exact solution in higher dimensions for wider range of $-U/t$ values.

### F. Order parameter

The order parameter $\Delta$ significantly imitates the behavior of parameter $D$ under the variation of $-U/t$ and $n$. From Eq. (30) we obtain a simple relationship:

$$\Delta = 2|U|\sqrt{D-D_0}. \tag{42}$$

Nonvanishing order parameter $\Delta$ in one dimension is an artifact of the SCF approach. Due to strong fluctuations only algebraically decaying correlations (Kosterlitz-Thouless type[37]) are expected, rather than true long-range order in one dimension. Thus the SCF order parameter $\Delta$ does not have corresponding analogue in the exact theory. Nevertheless it is interesting to compare the SCF result for $\Delta$ with the similar parameter, $\Delta_{ex} \equiv 2|U|\sqrt{D-D_0}$ defined in the exact theory to see how these two quantities are related to each another. In Fig. 14 we plot the variation of the order parameter $\Delta$, using the Eq. (42) along with the exact result for parameter $\Delta_{ex}$ as a function of $-U/t$ for various $n$. We notice that the exact parameter $\Delta_{ex}$ and the order parameter $\Delta$ show the perfect matching for various $n$ in wide range of $U/t$. In Fig. 14, both $\Delta$ and $\Delta_{ex}$ depend on $n$ and have a tendency to grow monotonously with increasing coupling strength $-U/t$. We can compare also the SCF results for $E_{gap}$ and $\Delta$ in Figs. 12 and 14 to see that these parameters nicely follow each other for small $U/t$ till the crossover (intersection with the bold curve $-U_c/t$), showing the onset of separation and difference between gap and order parameter. Note that at zero filling, $n=0$, the order parameter vanishes $\Delta=0$, whereas the SCF gap is equal to the exact gap $E_{gap}=\sqrt{U^2+16t^2}-4t$.[38,14] Thus the coupling strength $U/t \neq 0$ preserves the gap (electron binding), even though the pairing parameter $\Delta$ vanishes at zero band filling. The relationship in Eq. (30) along with the obtained results for $\Delta_{ex}$ and $\Delta$ show that parameters $D$ and $\Delta^2/4U^2$ have many common features in wide range of coupling strength $-U/t$.

Under the decreasing of $n$ the parameter $\Delta$ and $\Delta_{ex}$ both change as it is shown in Fig. 15. Here again we have a perfect agreement between $\Delta$ and $\Delta_{ex}$ for all band fillings $n$ and different $U/t$ values. In SCF approach there is an exact correspondence in behavior between $E_{gap}$ and $\Delta$ under the variation of band filling for large $n$ till the critical concentration $n_c$ shown in Figs. 13 and 15 by the bold curve. In general $\Delta$ is not a monotonous function of $n$. However, for $|U|/4t \geq 1$ the parameter $\Delta$ smoothly increases with $n$, and at relatively large $-U/t$ we have $\Delta=|U|\sqrt{n(2-n)}$.[32] For small $|U|/4t \leq 1$, the parameter $\Delta$ primary increases passing through maximum and then gradually decreases. Note that when the band filling $n \to 0$, the order parameter vanishes and the system with the empty band becomes insulator with the chemical potential disposed below the bottom of the conduction band, $\mu_{zero} < -2t$. The SCF theory with renormalized chemical potential provides a simple gap (or pseudogap at finite temperatures) in the absence of pair coherence between the pairs $\Delta=0$. Near this threshold the system behaves as an insulator with preformed bound pairs similar to what was found recently in high-$T_c$ cuprates in underdoped regime $n \to 0$.[28] The superconductivity occurs only when initially formed pairs become coherent $\Delta \neq 0$. Note that the order parameter is significantly suppressed ($\Delta \to 0$) near $n=0$, while $E_{gap}$ is relatively large. The SCF theory overestimates the value of the exact gap for all values of $-U/t$ and $n$, but it correctly describes the difference in behavior between the order parameter and excitation gap under the variation of $n$ and $-U/t$.

### G. Phase diagram

The crossover from Cooper pairing phase to Bose condensation phase as a function of $-U/t$ and $n$ within SCF ap-

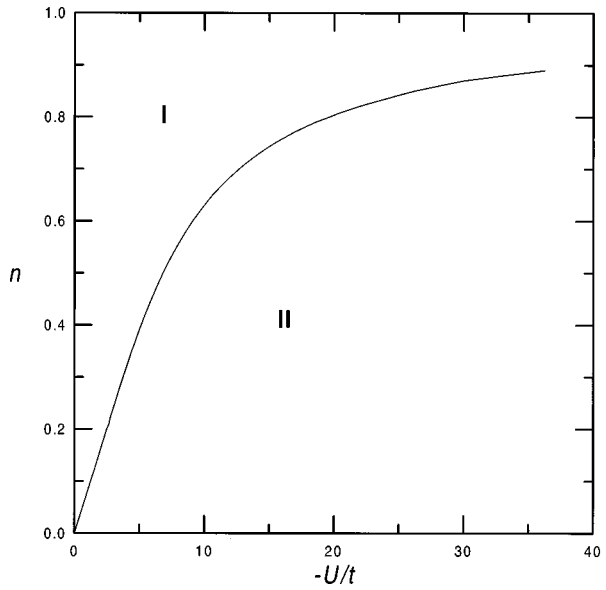


FIG. 16. The phase diagram of one-dimensional negative-$U$ Hubbard model in the SCF approach: in region I the minimum gap occurs at $k\neq 0$, in region II the minimum gap occurs at $k=0$.

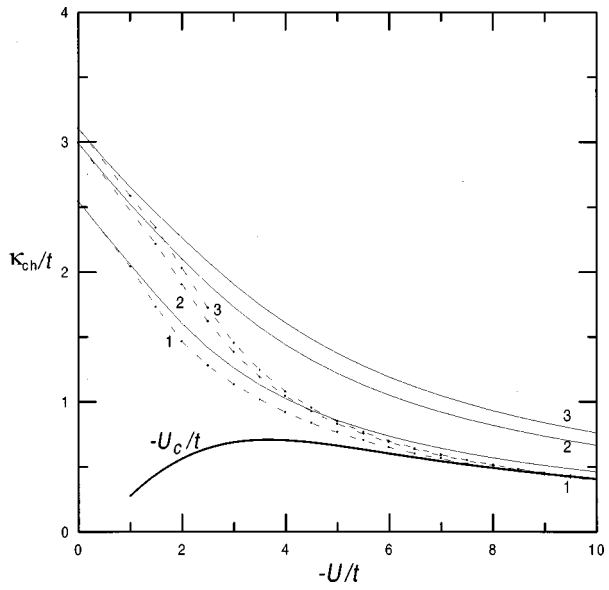


FIG. 17. The ground-state compressibility $\kappa_{\rm ch}$ as a function of $-U/t$ in the exact theory (solid curves) and the SCF approach (dots and dashed curves). Curve indexes 1–3 correspond to $n=0.6,0.8,0.9$.

proach in one dimension is smooth (i.e., there is no sharp distinction between these phases). The minimum gap at momentum $k=0$ serves as a measure to distinguish different regimes on the phase diagram, where either BCS-like or Bose condensation behavior take place. Figure 16 show the ground-state phase diagram in $n$-$U$ plane using our SCF results in one dimension. The energy gap on the Fermi surface $k\neq 0$ (at $\bar{\mu}>-2t$) everywhere in region I. In region II a gap in the spectrum occurs at the bottom of conduction band with zero momentum $k=0$ ($\bar{\mu}\leqslant -2t$) and the energy gap is different from the order parameter $\Delta$. The boundary between the region I and II, defined by Eq. (40), describes a smooth crossover from a picture of overlapping Copper pairs to the Bose condensate of independent local pairs with momentum $k=0$. The Bose condensation of preformed pairs in region II is driven by the coupling strength and band filling. For any infinitesimal small $|U|/t$ one can get a crossover from region I into II by the variation of $n$ that leads to the changeover to the BCS-like behavior. At large $|U|/t$ limit, the region I is gradually decreased and at relatively small deviation from half-filling gives a crossover from one regime to another, providing the separation of $\Delta$ from $E_{\rm gap}$. The smooth character of transition is confirmed by careful inspection in behavior of the ground-state energy $E_{\rm GS}$ and other quantities (see Secs. IV A and IV E) as functions of $-U/t$ and $n$.

Note that within the SCF approach there is no Bose condensation of electrons with momentum $k=0$ at the half-filled band ($n=1$) even for the large $|U|/t$ limit due to the effect of strong interaction between the local pairs. Thus the evolution from weakly bound BCS pairs to localized pairs at $n=1$ in the ground state within the SCF approach takes place without crossover. This interesting feature shows the difference in behavior between the discrete lattice at $n=1$ and continuum models.[13] Our conclusion about the crossover away from half-filling is overall in agreement with the previous studies of crossover in the one-dimensional continuum model.[23] Note that in region II near empty band $n=0$ there exists also a simple transition, driven by decreasing of $n$, from the Bose condensation regime into an insulating state with $\Delta=0$ and $E_{\rm gap}=-2\mu_{\rm zero}-4t$. Also we expect to get a similar phase diagram within the SCF approach in higher dimensions.

### H. Compressibility

The behavior of the compressibility $\kappa_{\rm ch}\equiv\partial\mu/\partial n$ (or charge susceptibility $\chi_{\rm ch}\equiv\partial n/\partial\mu=\kappa_{\rm ch}^{-1}$) is also a sensitive test for the estimation of the accuracy of the SCF theory.

In the exact theory, we can calculate $\kappa_{\rm ch}$ from corresponding integral equations (Appendix E). In the SCF approach $\kappa_{\rm ch}$ must be determined self-consistently (Appendix F). At half-filling we have in the exact theory[12]

$$\kappa_{\rm ch}|_{n\to 1}=\frac{t\pi I_1(-2\pi t/U)}{I_0(-2\pi t/U)}, \tag{43}$$

corresponding to zero-field spin susceptibility $\chi_{\rm ch}$ in the repulsive Hubbard model, $\chi_{\rm ch}=\kappa_{\rm ch}^{-1}$.[39]

Figures 17 and 18 show the variation of $\kappa_{\rm ch}$ as a function of $-U/t$ for different values $n$ both in the exact and SCF theories. As shown in Fig. 18 the SCF theory yields a finite value for compressibility at $n=0$, while the exact $\kappa_{\rm ch}\to 0$ ($\chi_{\rm ch}$ diverges).[10,12] We note that the SCF approach significantly underestimates $\kappa_{\rm ch}$ near half-filling ($n\to 1$) and overestimates it near the empty band filling ($n\to 0$). Nevertheless, the SCF result captures the general trend in behavior of $\kappa_{\rm ch}$ under the variation of $U/t$ and $n$. The discrepancy with the exact results decreases with decreasing of the interaction strength $-U/t$. One can see from Figs. 17 and 18 that the most serious errors occur at half-filling for large $-U/4t\geqslant 1$. The exact and SCF results are relatively close for $-U/t\leqslant 0.5$ and all $n$. The deviations clearly reveal that the fluctuations must be included beyond the SCF approach to obtain the better quantitative agreement for $\kappa_{\rm ch}$. In Figs. 17

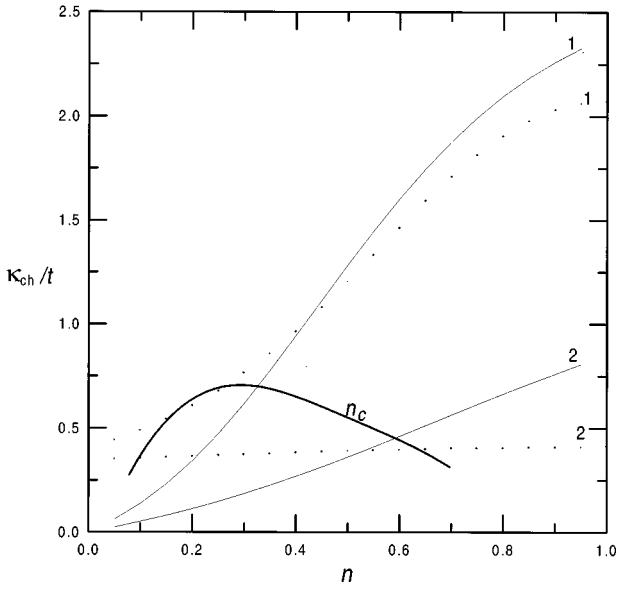


FIG. 18. The ground-state compressibility $\kappa_{ch}$ as a function of $n$ in the exact theory (solid curves) and the SCF approach (dots). Curve indexes 1,2 correspond to $-U/t=2.0,10.0$.

and 18 the crossover in $\kappa_{ch}$ from the BCS regime into the Bose condensation behavior under the variation of $-U/t$ and $n$ is also shown.

## V. SUMMARY

In this paper we solved numerically the Lieb-Wu equations and the self-consistent equations with a renormalized chemical potential for general band fillings $n$ and coupling strength $-U/t$. We compared in one dimension the exact and the SCF ground-state properties such as the energy, the concentration of the double occupied sites, the kinetic energy, and the chemical potential. In overall the SCF results show a good agreement with the exact results. The largest discrepancy occurs in the half-filling case and at the intermediate values of $-U/t$. Even at $n=1$ the results are very close to the exact values in the wide range of $-U/t$. The absolute and relative errors in the calculations of the energy $E_{GS}$ and the chemical potential $\mu$ for all $n$ values systematically decrease with increasing $-U/t$. The SCF approach at strong and weak coupling reproduces the exact results and gives a reasonable interpolation scheme for the intermediate region of $-U/t$.

Although the SCF approach is quite accurate in describing the ground-state properties, however, it poorly reproduces the characteristics of excited states. It fails to give the correct numerical values for the excitation gap $E_{gap}$ and it underestimates the compressibility $\kappa_{ch}$ at large $-U/t$ by a factor of $4/\pi^2$ at half-filling. The correlation effect in the SCF approach are seen to be underestimated for all calculated quantities of the weak-coupling regime $-U/4t<1$. At half-filling the SCF result for the concentration of the double occupied sites $D$ gives a good agreement with the exact one for $-U/4t\geqslant 1$. The SCF approach provides a simple analytical relationship between parameters $D$, $n$, and $\Delta$, valid for all $-U/t$ and $n$. The parameter $\Delta$ has physical meaning closely associated with parameter $D$, rather than $E_{gap}$. This conclusion is also based on the perfect agreement between the order parameter $\Delta$ in the SCF approach and a similar parameter $\Delta_{ex}=\sqrt{D-D_0}$ introduced in the exact theory.

The SCF approach at $n\neq 1$ suggests in one dimension a smooth crossover from the BCS limit to the ideal Bose gas of independent local pairs with zero momentum $k=0$, since there is only a weak singularity in the excitation spectrum at $\bar{\mu}=-2t$. The nonideal Bose gas behavior of local pairs is a characteristic feature of the discrete lattice model exactly at $n=1$. At half-filling the gap in spectrum is identical with $\Delta$ and the system remains in the BCS regime with the gap in momentum space at $k=\pi/2$ even at strong coupling. All physical quantities for various $n$ evolve smoothly with increasing $-U/t$ from the weak- to strong-coupling limit.

The weak singularity in the excitation spectrum at $n_c$ within the SCF approach reflects the difference between the order parameter $\Delta$ and the energy gap $E_{gap}$.

Thus the exact and SCF results both show that the ground-state properties change smoothly with $-U/t$ and there is no singular point in the $-U/t-n$ plane except for $n=1$ and $U=0$. In a future work we shall apply the Bethe-ansatz formalism to calculate the correlation functions to discover the difference and the relation between the unrenormalized Fermi momentum $k_F$ in a non-Fermi-liquid and the SCF parameter $k_0$.

The SCF theory shows also the interplay between the localization and superconductivity under the variation of band filling. Near empty band the system undergoes the transition from the Bose condensation regime into insulating state with the energy gap for preformed pairs without coherence ($\Delta=0$). We found that the energy gap $E_{gap}$ is a monotonous decreasing function of the doping level (band filling near $n=0$), while superconducting gap $\Delta$ is much smaller and in general follows the nonmonotonous trend of its critical temperature. The suppression of the superconductivity and preservation of the gap at vanishing concentration of carriers (or band filling) are consistent qualitatively with the structure of a gap (or pseudogap at finite temperatures) in overdoped regime seen recently in low-temperature tunneling experiments in YBCO and BSCCO.[40,41] The good agreement between the SCF and Bethe-ansatz results suggests the correct picture of the crossover even in one dimension at least in the low-density limit.

Although much theoretical effort has been devoted to the examining of the crossover in the exact approach, still not very much is known, in particular, about low-lying excitations and spectral properties of the attractive Hubbard model.[42] Our future studies will be focused on the problem of the crossover in higher dimensions and we expect that the SCF approach will be more accurate in two and three dimensions. We conclude that the SCF approach with a renormalized chemical potential in lattices retains the essential difference from the standard BCS approach for all $n\neq 1$.

## ACKNOWLEDGMENTS

A.N.K. is cordially thankful to Professor Jenn-An Lin for the invitation to visit Tamkang University and the hospitality extended to him during his visit there. The authors wish to acknowledge the National Science Council of R.O.C. for support (Grant No. NSC88-2112-M-032-011).

## APPENDIX A: CONCENTRATION OF DOUBLE OCCUPIED SITES IN THE EXACT THEORY

In the exact theory from Eq. (28) and Eqs. (18)–(24) we have for the concentration of double occupied sites

$$D=\frac{n}{2}-s-2\int_{-Q}^{Q}dk\rho_U(k)\cos k-4Q_U\rho(Q)\cos Q, \tag{A1}$$

where $\rho_U(k)\equiv t\partial\rho(k)/\partial U$ and $\sigma_U(\lambda)\equiv t\partial\sigma(\lambda)/\partial U$ satisfy the following integral equations

$$\begin{aligned}\rho_U(k)=&-\frac{U\cos k}{4t\pi}\int_{-B}^{B}d\lambda\sigma_U(\lambda)f_1(k,\lambda)\\&-\frac{\cos k}{2\pi}\int_{-B}^{B}d\lambda\sigma(\lambda)[f_1(k,\lambda)/2-(U/4t)^2f_1(k,\lambda)^2]\\&-\frac{U\cos k}{4t\pi}[f_1(k,B)+f_1(k,-B)]\sigma(B)B_U,\end{aligned} \tag{A2}$$

$$\begin{aligned}\sigma_U(\lambda)=&-\frac{U}{4t\pi}\int_{-Q}^{Q}dk\rho_U(k)f_1(k,\lambda)\\&+\frac{U}{2t\pi}\int_{-B}^{B}d\lambda'\sigma_U(\lambda')f_2(\lambda,\lambda')\\&-\frac{1}{2\pi}\int_{-Q}^{Q}dk\rho(k)[f_1(k,\lambda)/2-(U/4t)^2f_1(k,\lambda)^2]\\&+\frac{1}{\pi}\int_{-B}^{B}d\lambda'\sigma(\lambda')[f_2(\lambda,\lambda')/2\\&-(U/2t)^2f_2(\lambda,\lambda')^2]\\&-\frac{U}{4t\pi}[f_1(Q,\lambda)+f_1(-Q,\lambda)]\rho(Q)Q_U\\&+\frac{U}{2t\pi}[f_2(\lambda,B)+f_2(\lambda,-B)]\sigma(B)B_U,\end{aligned} \tag{A3}$$

and $Q_U\equiv t\partial Q/\partial U$, $B_U\equiv t\partial B/\partial U$ are determined from the relations

$$\int_{-Q}^{Q}\rho_U(k)dk+2\rho(Q)Q_U=0, \tag{A4}$$

$$\int_{-B}^{B}\sigma_U(\lambda)d\lambda+2\sigma(B)B_U=0. \tag{A5}$$

The functions $f_1(k,\lambda)$ and $f_2(\lambda,\lambda')$ are defined by Eqs. (21) and (22).

Substituting the solution of the integral Bethe-ansatz equations (18)–(24) into Eqs. (A1)–(A5) and resolving these equations we obtain the concentration of the double occupied sites $D$ as a function of $-U/t$, $n$, and $s$. At $s=0$ we have the ground state $D$ (in this case $Q_U=0$).

## APPENDIX B: KINETIC ENERGY IN THE EXACT THEORY

In the exact theory for the kinetic energy we have from Eqs. (33) and (18)–(24)

$$E_{\rm kin}=-2t\int_{-Q}^{Q}dk[\rho(k)+\rho_t(k)]\cos k-4tQ_t\rho(Q)\cos Q, \tag{B1}$$

where $\rho_t(k)\equiv t\partial\rho(k)/\partial t$ and $\sigma_t(\lambda)\equiv t\partial\sigma(\lambda)/\partial t$ satisfy the following integral equations

$$\begin{aligned}\rho_t(k)=&-\frac{U\cos k}{4t\pi}\int_{-B}^{B}d\lambda\sigma(\lambda)[f_1(k,\lambda)\\&-2(\lambda-\sin k)^2f_1(k,\lambda)^2]\\&-\frac{U\cos k}{4t\pi}\int_{-B}^{B}d\lambda\sigma_t(\lambda)f_1(k,\lambda)\\&-\frac{U\cos k}{4t\pi}[f_1(k,B)+f_1(k,-B)]\sigma(B)B_t,\end{aligned} \tag{B2}$$

$$\begin{aligned}\sigma_t(\lambda)=&-\frac{U}{4t\pi}\int_{-Q}^{Q}dk\rho(k)[f_1(k,\lambda)\\&-2(\lambda-\sin k)^2f_1(k,\lambda)^2]\\&+\frac{U}{2t\pi}\int_{-B}^{B}d\lambda'\sigma(\lambda')[f_2(\lambda,\lambda')\\&-2(\lambda-\lambda')^2f_2(\lambda,\lambda')^2]\\&-\frac{U}{4t\pi}\int_{-Q}^{Q}dk\rho_t(k)f_1(k,\lambda)\\&+\frac{U}{2t\pi}\int_{-B}^{B}d\lambda'\sigma_t(\lambda')f_2(\lambda,\lambda')\\&-\frac{U}{4t\pi}[f_1(Q,\lambda)+f_1(-Q,\lambda)]\rho(Q)Q_t\\&+\frac{U}{2t\pi}[f_2(\lambda,B)+f_2(\lambda,-B)]\sigma(B)B_t,\end{aligned} \tag{B3}$$

and $Q_t\equiv t\partial Q/\partial t$, $B_t\equiv t\partial B/\partial t$ are determined from the relations

$$\int_{-Q}^{Q}\rho_t(k)dk+2\rho(Q)Q_t=0, \tag{B4}$$

$$\int_{-B}^{B}\sigma_t(\lambda)d\lambda+2\sigma(B)B_t=0. \tag{B5}$$

Equations (18)–(24) and (B1)–(B5) determine $E_{\rm kin}$ as a function of $-U/t$, $n$, and $s$. At $s=0$ we have the ground state $E_{\rm kin}$ (in this case $Q_t=0$).

## APPENDIX C: CHEMICAL POTENTIAL IN THE EXACT THEORY

In the exact theory the chemical potential is

$$\mu=\frac{U}{2}-2t\int_{-Q}^{Q}dk\rho_n(k)\cos k-4tQ_n\rho(Q)\cos Q, \quad \text{(C1)}$$

where $\rho_n(k)\equiv\partial\rho(k)/\partial n$ and $\sigma_n(\lambda)\equiv\partial\sigma(\lambda)/\partial n$ satisfy the following integral equations:

$$\rho_n(k)=-\frac{U\cos k}{4t\pi}\int_{-B}^{B}d\lambda\sigma_n(\lambda)f_1(k,\lambda)-\frac{U\cos k}{4t\pi}[f_1(k,B)+f_1(k,-B)]\sigma(B)B_n, \quad \text{(C2)}$$

$$\sigma_n(\lambda)=-\frac{U}{4t\pi}\int_{-Q}^{Q}dk\rho_n(k)f_1(k,\lambda)+\frac{U}{2t\pi}\int_{-B}^{B}d\lambda'\sigma_n(\lambda')f_2(\lambda,\lambda')-\frac{U}{4t\pi}[f_1(Q,\lambda)+f_1(-Q,\lambda)]\rho(Q)Q_n+\frac{U}{2t\pi}[f_2(\lambda,B)+f_2(\lambda,-B)]\sigma(B)B_n, \quad \text{(C3)}$$

and $Q_n\equiv\partial Q/\partial n$, $B_n\equiv\partial B/\partial n$ are determined from the relations

$$\int_{-Q}^{Q}\rho_n(k)dk+2\rho(Q)Q_n=0, \quad \text{(C4)}$$

$$\int_{-B}^{B}\sigma_n(\lambda)d\lambda+2\sigma(B)B_n=\tfrac{1}{2}. \quad \text{(C5)}$$

Equations (18)–(24) and (C1)–(C5) determine $\mu$ as a function of $-U/t$, $n$, and $s$. At $s=0$ we have the ground state $\mu$ (in this case $Q_n=0$).

## APPENDIX D: ENERGY GAP IN THE EXACT THEORY

In the exact theory the energy gap is

$$E_{\text{gap}}=-U-2t\int_{-Q}^{Q}dk\rho_s(k)\cos k-4tQ_s\rho(Q)\cos Q, \quad \text{(D1)}$$

where $\rho_s(k)\equiv\partial\rho(k)/\partial s$ and $\sigma_s(\lambda)\equiv\partial\sigma(\lambda)/\partial s$ satisfy the following integral equations:

$$\rho_s(k)=-\frac{U\cos k}{4t\pi}\int_{-B}^{B}d\lambda\sigma_s(\lambda)f_1(k,\lambda)-\frac{U\cos k}{4t\pi}[f_1(k,B)+f_1(k,-B)]\sigma(B)B_s, \quad \text{(D2)}$$

$$\sigma_s(\lambda)=-\frac{U}{4t\pi}\int_{-Q}^{Q}dk\rho_s(k)f_1(k,\lambda)+\frac{U}{2t\pi}\int_{-B}^{B}d\lambda'\sigma_s(\lambda')f_2(\lambda,\lambda')-\frac{U}{4t\pi}[f_1(Q,\lambda)+f_1(-Q,\lambda)]\rho(Q)Q_s+\frac{U}{2t\pi}[f_2(\lambda,B)+f_2(\lambda,-B)]\sigma(B)B_s, \quad \text{(D3)}$$

and $Q_s\equiv\partial Q/\partial s$, $B_s\equiv\partial B/\partial s$ are determined from the relations

$$\int_{-Q}^{Q}\rho_s(k)dk+2\rho(Q)Q_s=-2, \quad \text{(D4)}$$

$$\int_{-B}^{B}\sigma_s(\lambda)d\lambda+2\sigma(B)B_s=-1. \quad \text{(D5)}$$

Equations (18)–(24) and (D1)–(D5) at $s=0$ determine $E_{\text{gap}}$ as a function of $-U/t$ and $n$.

## APPENDIX E: COMPRESSIBILITY IN THE EXACT THEORY

In the exact theory the compressibility is

$$\kappa_{\text{ch}}\equiv\frac{\partial\mu}{\partial n}\equiv\mu_n, \quad \text{(E1)}$$

$$\mu_n=-2t\int_{-Q}^{Q}dk\rho_{nn}(k)\cos k-8tQ_n\rho_n(Q)\cos Q-4tQ_{nn}\rho(Q)\cos Q+4tQ_n^2\left[\rho(Q)\sin Q-\left.\frac{\partial\rho(k)}{\partial k}\right|_{k=Q}\cos Q\right], \quad \text{(E2)}$$

where $\rho_{nn}(k)\equiv\partial\rho_n(k)/\partial n$ and $\sigma_{nn}(\lambda)\equiv\partial\sigma_n(\lambda)/\partial n$ satisfy the following integral equations

$$\rho_{nn}(k)=-\frac{U\cos k}{4t\pi}\int_{-B}^{B}d\lambda\sigma_{nn}(\lambda)f_1(k,\lambda)-\frac{U\cos k}{2t\pi}[f_1(k,B)+f_1(k,-B)]\sigma_n(B)B_n-\frac{U\cos k}{4t\pi}\left[\frac{\partial f_1(k,B)}{\partial B}+\frac{\partial f_1(k,-B)}{\partial B}\right]\sigma(B)B_n^2-\frac{U\cos k}{4t\pi}[f_1(k,B)+f_1(k,-B)]\left(\left.\frac{\partial\sigma(\lambda)}{\partial\lambda}\right|_{\lambda=B}\right)B_n^2-\frac{U\cos k}{4t\pi}[f_1(k,B)+f_1(k,-B)]\sigma(B)B_{nn}, \quad \text{(E3)}$$

$$\sigma_{nn}(\lambda)=-\frac{U}{4t\pi}\int_{-Q}^{Q}dk\rho_{nn}(k)f_1(k,\lambda)+\frac{U}{2t\pi}\int_{-B}^{B}d\lambda'\sigma_{nn}(\lambda')f_2(\lambda,\lambda')-\frac{U}{2t\pi}[f_1(Q,\lambda)+f_1(-Q,\lambda)]\rho_n(Q)Q_n$$
$$+\frac{U}{t\pi}[f_2(\lambda,B)+f_2(\lambda,-B)]\sigma_n(B)B_n-\frac{U}{4t\pi}\left[\frac{\partial f_1(Q,\lambda)}{\partial Q}+\frac{\partial f_1(-Q,\lambda)}{\partial Q}\right]\rho(Q)Q_n^2$$
$$-\frac{U}{4t\pi}[f_1(Q,\lambda)+f_1(-Q,\lambda)]\left(\left.\frac{\partial\rho(k)}{\partial k}\right|_{k=Q}\right)Q_n^2-\frac{U}{4t\pi}[f_1(Q,\lambda)+f_1(-Q,\lambda)]\rho(Q)Q_{nn}$$
$$+\frac{U}{2t\pi}\left[\frac{\partial f_2(\lambda,B)}{\partial B}+\frac{\partial f_2(\lambda,-B)}{\partial B}\right]\sigma(B)B_n^2+\frac{U}{2t\pi}[f_2(\lambda,B)+f_2(\lambda,-B)]\left(\left.\frac{\partial\sigma(\lambda)}{\partial\lambda}\right|_{\lambda=B}\right)B_n^2$$
$$+\frac{U}{2t\pi}[f_2(\lambda,B)+f_2(\lambda,-B)]\sigma(B)B_{nn}, \tag{E4}$$

and $Q_{nn}\equiv\partial Q_n/\partial n$, $B_{nn}\equiv\partial B_n/\partial n$ are determined from the relations

$$\int_{-Q}^{Q}\rho_{nn}(k)dk+4\rho_n(Q)Q_n+2\left(\left.\frac{\partial\rho(k)}{\partial k}\right|_{k=Q}\right)Q_n^2$$
$$+2\rho(Q)Q_{nn}=0, \tag{E5}$$

$$\int_{-B}^{B}\sigma_{nn}(\lambda)d\lambda+4\sigma_n(B)B_n+2\left(\left.\frac{\partial\sigma(\lambda)}{\partial\lambda}\right|_{\lambda=B}\right)B_n^2$$
$$+2\sigma(B)B_{nn}=0. \tag{E6}$$

Equations (18)–(24) and (E1)–(E6) determine $\kappa_{\rm ch}$ as a function of $-U/t$, $n$, and $s$. At $s=0$ we have the ground state $\kappa_{\rm ch}$ (in this case $Q_n=Q_{nn}=0$).

## APPENDIX F: COMPRESSIBILITY IN THE SCF APPROACH

In the SCF approach the compressibility $\kappa_{\rm ch}\equiv\partial\mu/\partial n\equiv\mu_n$ satisfies the following self-consistent equations

$$-\frac{1}{N_{\rm latt}}\sum_k\frac{(U-2\mu_n)E_k-2(E_k)_n(\varepsilon_k-\bar{\mu})}{2E_k^2}=1, \tag{F1}$$

$$\sum_k\frac{(E_k)_n}{E_k^2}=0, \tag{F2}$$

where

$$(E_k)_n\equiv\frac{\partial E_k}{\partial n}=\frac{2(\varepsilon_k-\bar{\mu})(U-2\mu_n)+\Delta\Delta_n}{4E_k}, \tag{F3}$$

and $\bar{\mu}\equiv\mu-nU/2$, $\Delta_n\equiv\partial\Delta/\partial n$.

Equations (15)–(16) and (F1)–(F3) determine self-consistently ground state $\mu$, $\Delta$, $\kappa_{\rm ch}$, and $\Delta_n$ as functions of $-U/t$ and $n$.


[1] D. W. Huang, Chin. J. Phys. **33**, 363 (1995).
[2] J. Bardeen, L. N. Cooper, and J. R. Schrieffer, Phys. Rev. **108**, 1175 (1957).
[3] L. P. Gor'kov, Sov. Phys. JETP **7**, 505 (1058).
[4] V. J. Emery, Phys. Rev. B **14**, 2989 (1976).
[5] R. Micnas, J. Ranninger, and S. Robaskiewicz, Rev. Mod. Phys. **62**, 113 (1990).
[6] A. N. Kocharian and C. Yang, Mater. Chem. Phys. **42**, 134 (1995).
[7] S. A. Kivelson and V. J. Emery, Report No. BN-61338 (unpublished).
[8] Ph. B. Allen, in *Electron Pairing: How and Why?* edited by J. W. Lynn, High Temperature Superconductivity (Springer-Verlag, Berlin, 1990), Chap. 9, p. 303.
[9] E. H. Lieb and F. Y. Wu, Phys. Rev. Lett. **20**, 1445 (1968).
[10] M. Takahashi, Prog. Theor. Phys. **42**, 1098 (1969); **44**, 348 (1970).
[11] V. Ya. Krivnov and A. A. Ovchinnikov, Sov. Phys. JETP **40**, 781 (1975).
[12] T. B. Bahder and F. Woynarovich, Phys. Rev. B **33**, 2114 (1986).
[13] R. M. Quick, C. Esebbag, and M. de Llano, Phys. Rev. B **47**, 11 512 (1993).
[14] F. Marsiglio, Phys. Rev. B **55**, 575 (1997).
[15] P. Nozieres and S. Schmitt-Rink, J. Low Temp. Phys. **59**, 195 (1985).
[16] A. J. Leggett, J. Phys. (Paris), Colloq. **41**, C7-19 (1980); in *Modern Trends in the Theory of Condensed Matter*, edited by S. Pekalski and J. Przystawa (Springer, Berlin, 1980), p. 13.
[17] M. Randeria, N. Trivedi, A. Moreo, and R. T. Scalettar, Phys. Rev. Lett. **69**, 2001 (1992).
[18] M. Randeria, J. M. Duan, and L. Y. Shieh, Phys. Rev. Lett. **62**, 981 (1989); Phys. Rev. B **41**, 327 (1990).
[19] J. Luo and N. E. Bickers, Phys. Rev. B **48**, 15 983 (1993).
[20] N. Kawakami and A. Okiji, Phys. Rev. B **40**, 7066 (1989).

[21] H. Shiba and P. Pincus, Phys. Rev. B **5**, 1966 (1972).
[22] K. J. B. Lee and P. Schlottmann, Phys. Rev. B **38**, 11 566 (1988); **40**, 9104 (1989).
[23] M. Cesas, C. Esebbag, A. Extremera, J. M. Getino, M. D. Lilano, A. Plastino, and H. Rubio, Phys. Rev. A **44**, 4915 (1991).
[24] J. M. Tranquada, Physica B **241**, 745 (1997).
[25] V. J. Emery and S. A. Kivelson, Physica C **209**, 597 (1993); **282-287**, 174 (1997).
[26] V. J. Emery and S. A. Kivelson, J. Phys. Chem. Solids **59**, 1705 (1998).
[27] A. G. Loeser *et al.*, Science **273**, 325 (1996).
[28] H. Ding *et al.*, Nature (London) **382**, 51 (1996).
[29] C. Kittel, *Quantum Theory of Solids* (Wiley, New York, 1987).
[30] E. M. Lifshits and L. P. Pitaevskii, *Statistical Physics, Part II*, (Pergamon, New York, 1980), Chap. V.
[31] W. H. Press *et al.*, *Numerical Recipes in Fortran*, 2nd ed. (Cambridge University Press, New York, 1992).
[32] S. Robaszkiewicz, R. Micnas, and K. A. Chao, Phys. Rev. B **23**, 1447 (1981).
[33] A. N. Kocharian, A. K. Jermakian, and C. Yang, Physica B **230-232**, 918 (1997).
[34] M. Takahashi, Prog. Theor. Phys. **43**, 917 (1970).
[35] I. Affleck, D. Gepner, and H. J. Schulz, J. Phys. A **22**, 511 (1989); M. Yamanaka, M. Oshikawa, and I. Affleck, Phys. Rev. Lett. **79**, 1110 (1997).
[36] T. Pruschke and H. Shiba, Phys. Rev. B **44**, 205 (1991).
[37] J. Kosterlitz and D. Thouless, J. Phys. C **6**, 1181 (1973).
[38] J. E. Hirsch, Physica C **179**, 317 (1991).
[39] M. Takahashi, Prog. Theor. Phys. **43**, 1619 (1970).
[40] A. Matsuda, S. Sugita, and T. Watanabe, Bull. Am. Phys. Soc. **43**, 665 (1998).
[41] A. Gupta, Bull. Am. Phys. Soc. **43**, 666 (1998).
[42] F. Woynarovich, J. Phys. C **16**, 6593 (1983).